Rheological Analysis of Surface Relaxation Process of Monodisperse Polystyrene Films

Keiji Tanaka, Atsushi Takahara,† and Tisato Kajiyama*

Department of Applied Chemistry, Faculty of Engineering, Kyushu University, Fukuoka 812-8581, Japan

Received March 6, 2000; Revised Manuscript Received July 10, 2000

ABSTRACT: Surface glass transition temperature, T_g^s, of monodisperse polystyrene (PS) films was determined from the temperature dependence of lateral force at a given scanning rate. The end groups of the PS were composed of *sec*-butyl group and a repeating unit terminated by proton. T_g^s of the PS films was discerned to be markedly lower than its bulk T_g, T_g^b, in the entire number-average molecular weight, M_n, range, 4.9K to 1460K. The M_n dependence of T_g^s was analyzed on the basis of a simple power law. The exponent of M_n related to T_g^s was -0.60 ± 0.03 in contrast to the power of -0.5 from the Mayes scaling argument that is based on both chain ends being perfectly localized at the surface. This result implies that the surface localization of end groups of the PS used here is not complete. The T_g^s extrapolated to the infinite M_n was found to be lower than the corresponding T_g^b by approximately 20 K. The apparent activation energy of the surface α_a-relaxation process for the PS obtained from Arrhenius plot was 230 ± 10 kJ·mol^{-1}, significantly smaller than that for the bulk PS. Also, it was shown on the basis of Ngai's coupling model that the cooperative motion at the surface can be achieved much easier than its internal bulk phase. Thus, the difference between the T_g^s and the T_g^b for the infinite M_n PS was explained in terms of the size and/or energy barrier reduction of the cooperative movement for the surface α_a-relaxation process, which might be arisen from the existence of the free space presented to polymer segments at the surface.

Introduction

Surfaces and interfaces of polymeric materials play an important role in many technological applications such as lubrication, adhesion, and biomaterials.[1] To design highly functionalized polymeric materials, the systematical understanding of aggregation states and physical properties in the vicinity of surface and interfacial layers, which are impossible to be deduced only by extrapolating the bulk ones, is of pivotal importance as the first benchmark.

Since the early 1990s, thermal behaviors in polymer thin films have been extensively explored with the advent of modern spectroscopic and microscopic methods. Restricting ourselves to the discussion of polystyrene (PS) for brevity, a conclusion obtained is consistently arrived that the glass transition temperature, T_g, in thin films differs markedly from that for the bulk, although the interpretations as to why T_g must be lowered in thin films differ.[2−7] It seems to us that the most persuasive arguments with respect to a depression of T_g in thin films are based on the specific thermal behaviors of polymer chains around surface and interfacial regions.

Authors have systematically embarked on surface molecular motions of PS films mainly by scanning force microscopy, e.g., scanning viscoelasticity[8−11] and lateral force microscopy [12−14] (SVM and LFM). SVM enables one to gain direct access to viscoelastic properties on solid surfaces by measuring an amplitude change in response force, and detecting a phase lag between a stimulus displacement and a response force. [8,10] LFM relies on a measure of lateral force between a sample surface and a probe tip, and has been demonstrated to be a powerful tool to investigate viscoelasticity of various polymer surfaces. [12−16] The authors have found that in the case of the monodisperse PS film with a number-average molecular weight, M_n, smaller than ca. 40K, the surface was in the glass to rubber transition state or rubbery state at room temperature even though the bulk glass transition temperature, T_g^b, was far above the room temperature. [9−11] Furthermore, the thermal molecular motion of polymer chains at the surface was strongly influenced by chemical structures of chain end groups.[13] Boiko and Prud'homme, using lap-shear strength measurements, observed that the strength at PS/PS interface developed due to interdiffusion of PS chains at a temperature below T_g^b, and concluded that the mobility at the free surface was highly enhanced in comparison with its internal bulk state.[17] Besides, positron-annihilation spectroscopic studies clearly indicated that T_g in the thin surface layer of PS film was suppressed.[18] On the other hand, these conclusions are in contrast to a recent report on surface relaxation of PS film with M_n of 96K, based on the spectroscopy of near-edge X-ray absorption fine structure by Liu et al.[19] They have not observed any evidence of vigorous molecular motion on PS film surface at temperatures below its T_g^b. Hence, it seems that a consensus for the thermal molecular motions at the film surface is yet to emerge.

The objective of this study is to elucidate the thermal molecular motions at the surface of the monodisperse PS films based on LFM measurement at various sample deformation rates and temperatures. Specifically, our intent in this paper is to describe the molecular weight dependence of surface glass transition temperature,

* To whom correspondence should be addressed. Fax: +81-92-651-5606. Telephone: +81-92-642-3558. E-mail: kajiyama@cstf.kyushu-u.ac.jp.

† Current address: Institute for Fundamental Research of Organic Chemistry, Kyushu University.

10.1021/ma000406w CCC: $19.00
Published on Web 09/14/2000

T_g^s, of the PS films, and bring for the factors influencing T_g^s.

Experimental Section

Monodisperse PSs with various M_ns were synthesized by the anionic polymerization method using *sec*-butyllithium and methanol as an initiator and a terminator, respectively. Hence, the chemical structures at the chain ends are composed of a *sec*-butyl group and a repeating unit terminated by proton. The PS film was coated from a toluene solution onto a cleaned silicon wafer by a spin-coating method. The film was dried at 296 K for more than 24 h and then annealed at 393 K for 24 h under vacuum. The film thickness evaluated by ellipsometric measurement was approximately 200 nm, which was sufficient to avoid any ultrathinning effects on the surface molecular motion.

The surface relaxation behavior of the PS film was examined by using LFM (SPA 300 HV, Seiko Instruments Industry Co., Ltd.) with an SPI 3800 controller. LFM measurements were carried out at various temperatures in vacuo so as to avoid the surface oxidation and a capillary force effect induced by surface-adsorbed water. A piezoscanner was thermally insulated from the heating stage. A cantilever with the bending spring constant of 0.09 $N \cdot m^{-1}$, of which both sides were uncoated or coated by gold, was used. The applied force to the cantilever tip was set to be 10 nN in a repulsive force region. It was confirmed that the sample surface was not damaged at all by scanning the tip under the current experimental condition. T_g^b was determined by differential scanning calorimetry (DSC8230, Rigaku Co., Ltd.). The specimen was heated to 423 K at a heating rate of 10 $K \cdot min^{-1}$ under dried nitrogen purge.

Results and Discussion

Since the frictional behavior of polymeric solids is closely related to their viscoelastic properties,[20] it is possible to examine surface molecular motion of the polymeric solids by using LFM, which is a powerful tool to detect lateral force between sliding cantilever tip and solid surface on a nanometer scale. What is central to our claim is that the lateral force alteration with measuring temperature and scanning rate corresponds well to the temperature and frequency dependences of dynamic loss modulus, respectively.[10,16] In either case that the surface is completely in a glassy or rubbery state, the magnitude of lateral force is not strongly dependent on the measuring temperature at a given scanning rate or the scanning rate at a given temperature. On the contrary, the lateral force discernibly varies with the temperature or the scanning rate, and a peak is observable on the lateral force−temperature or the lateral force−scanning rate curve when the surface is in a glass−rubber transition state. Hence, if the lateral force changes with the temperature or the scanning rate, it can be judged that the surface is in a glass−rubber transition state. Since the frequency range of our LFM is restricted within a few decades, it is impossible to obtain the whole picture of surface relaxation phenomena from a glassy to a rubbery state at a given temperature. Thus, the lateral force measurement was made at various temperatures as well as different scanning rates in order to apply the time−temperature superposition principle to the surface molecular motion.

Figure 1 shows the lateral force vs temperature curves for the PS films with M_n of 4.9K and 140K at a fixed scanning rate, v, of 10^3 $nm \cdot s^{-1}$. The ordinate is normalized by the peak value of lateral force to show how the lateral force varies with temperature in the vicinity of a transition region. The lateral force−temperature curves shown in Figure 1 make it clear that each surface transition temperature for the PS films with M_n of 4.9K and 140K is much lower than their T_g^b of 348 and 376 K, respectively, based on the onset of DSC curves, at which the heat capacitance starts to increase. Thus, it seems reasonable to conclude that the thermal molecular motions at PS film surfaces are more activated than those in the internal bulk phase. The activation has been hitherto attributed to the surface localization of chain end groups, both experimentally[9−14] and theoretically,[21] which might induce an extra free volume at the surface.

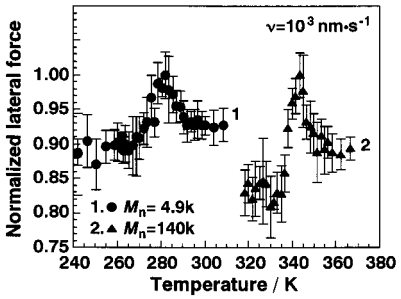

Figure 1. Typical lateral force−temperature curves at a given scanning rate. The curves for the PSs with M_n of 4.9K and 140K at the scanning rate of 10^3 $nm \cdot s^{-1}$ are displayed. The T_g^b values measured by DSC were 348 and 376 K, respectively.

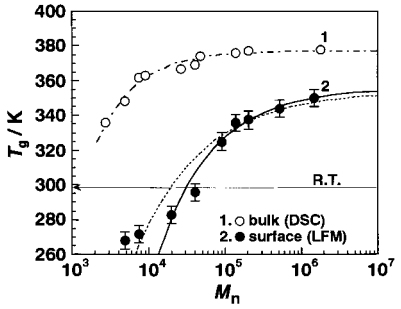

Figure 2. Molecular weight dependences of T_g^b and T_g^s of the monodisperse PS, which were determined by DSC and LFM, respectively. The arrow beside the ordinate shows the room temperature. The dotted curve traces the T_g^s variations with M_n deduced by Mayes' scaling theory, whereas the solid curves are drawn in the context of the power law analysis.

An onset temperature on the lateral force−temperature curve, that is, the temperature at which the magnitude of lateral force starts to increase, can be empirically defined as T_g^s. Figure 2 shows T_g^s so obtained as a function of M_n, and T_g^b determined by DSC are also plotted. The arrow beside the ordinate denotes our room temperature, which is abbreviated as "R.T.". It is clear that T_g^s exhibits a stronger M_n dependence than T_g^b. While T_g^b monotonically decreases with M_n, consistent with the empirical equation established by Fox and Flory,[22] there seems two regions where the M_n dependence of T_g^s differs, as shown in Figure 2. A possible explanation of such a relation of T_g^s to M_n at a lower M_n, roughly bordered by $M_n = 20$K, is deferred to later section. Even at ultrahigh molecular weight, $M_n = 1450$K, the T_g^s was definitely lower than the T_g^b. Besides, the film surface was already in a glass−rubber transition or rubbery state at room temperature in the case of M_n smaller than approximately 40K. These results are in good accord with our parallel experiment by using another technique, scanning viscoelasticity microscopy.[23]

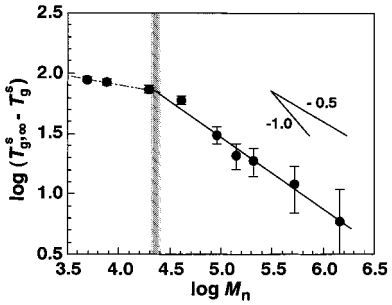

Figure 3. Double-logarithmic plot of $(T_{g,\infty}^s - T_g^s)$ vs M_n for the monodisperse PS in accord with a power law analysis. Two slopes of −0.5 and −1.0 are inserted to make the comparison with that obtained experimentally easy. The shaded region identifies the crossover between different M_n dependences of T_g^s.

According to Mayes' scaling theory[21] invoking that the chain end localization at the surface is perfect, the M_n dependence of T_g^s is given by

$$T_g^s = T_{g,\infty} - K_M(b/d)\, M_n^{-0.5} \qquad (1)$$

where $T_{g,\infty}$ is the glass transition temperature for a chain with the infinite M_n, b is the statistical segment length, d is the depth from the outermost surface, and K_M is a material constant. The dotted curve in Figure 2 was drawn based on eq 1 with $K_M = 1.12 \times 10^4$,[22] $b =$ 0.68 nm,[24] $d = 1$ nm, and the $T_{g,\infty}$ of 354 K as a fitting parameter. This $T_{g,\infty}$ of 354 K would correspond to the $T_{g,\infty}$ at the surface, $T_{g,\infty}^s$, and is much lower than the $T_{g,\infty}^b$ of 378 K. Although eq 1 with the $T_{g,\infty}^s$ of 354 K reproduces quite well the experimental T_g^s at a M_n higher than 10^5, this is not the case for a shorter PS chain. Hence, another method is applied to understand the dependence of T_g^s on M_n. Given that T_g^s is represented by the analogous equation with eq 1, it can be examined how T_g^s relates to M_n.

$$T_g^s = T_{g,\infty}^s - KM_n^{\alpha} \qquad (2)$$

Here α and K are constants. Figure 3 shows a double-logarithmic plot of $(T_{g,\infty}^s - T_g^s)$ against M_n to extract the power of M_n. When log M_n reaches approximately 4.3, the slope of the linear relation between $\log(T_{g,\infty}^s - T_g^s)$ and log M_n changes. The solid line drawn in Figure 3 indicates the best fitted one with the $T_{g,\infty}^s$ of 356 K as a fitting parameter, provided that the two data points at the smaller M_n side were not counted due to its apparent deviation from the linear relationship. Thereby the $T_{g,\infty}^s$ for the PS inferred from eq 2 was again definitely lower than the $T_{g,\infty}^b$ of 378 K. For the PS with the infinite M_n, the number density of chain end groups on the surface is negligible. Nevertheless, the glass transition temperature was lowered even at such a pristine surface. Thus, it is conceivable that the surface molecular motion is activated by other factors in addition to the surface localization of chain end groups. Since there is the free space on the polymer surface, it seems most likely that the size and/or energy barrier of the cooperative movement related to the micro-Brownian motion is reduced at the surface, resulting in the T_g difference between at the surface and in bulk even for the infinite longer PS chain. Also the segment density in the vicinity of the outermost surface might become smaller, as claimed in the intriguing simulation reports.[25−27] Furthermore, the chain entanglement has been inferred to be depressed at the surface region.[28] These factors are also possible to be the reason why $T_{g,\infty}^s$ is lower than $T_{g,\infty}^b$.

The slope of the best fitted line in Figure 3 was −0.6 ± 0.03, which was somewhat different from Mayes' value of −0.5 in eq 1. Since the power of −0.5 was derived on the basis of the assumption that both chain ends were perfectly localized at the film surface, our result implies that the surface segregation of end groups for the PS is far from complete. This conclusion corresponds well to our previous findings. The T_g^s depression of PS terminated by fluoroalkyl groups was larger than that of the proton-terminated PS owing to the more remarkable surface localization of chain ends, whereas in the case of PS terminated by hydrophilic amino groups, a decrement of T_g^s was smaller than that for the corresponding proton-terminated PS.[23] Besides, it should be worthwhile to note that our exponent of M_n against T_g^s is fairly close to the M_n power of $-2/3$ in the relation of surface tension against M_n, which has been explained in terms of the chain end effect as well.[29] At the present time, it is hard to conclude whether this apparent agreement of the M_n exponent between T_g^s and the surface tension occurs by accident or whether there exists a universal M_n dependence on the surface physical properties, as seen in the established physical properties for bulk amorphous polymers; e.g., T_g, the thermal expansion coefficient, and specific gravity are inversely proportional to M_n.[30] Unfortunately, the physical meaning of a gentle slanting slope obtained at the smaller M_n region bordered by $10^{4.3}$ is not clear either for the moment. The solid curve in Figure 2 was drawn from the eq 2 with $\alpha = -0.6$ and $T_{g,\infty}^s = 356$ K.

Once log M_n falls short of the crossover region identified by the shaded area in Figure 3, the slope of the linear dependence of $\log(T_{g,\infty}^s - T_g^s)$ on log M_n is varied. This is presumably due to the discrepancy in chain conformation at the surface between the two different M_n ranges. In the case of a PS with larger M_n, it might be possible for most of the chain ends to orient to the surface if the surface free energy of end groups is small enough to allow them to segregate to the surface. On the other hand, this would not be true for a shorter chain because the chain would suffer too large a loss in entropy on account of its smaller internal freedom if the most chain ends are localized at the surface. This means that an increment of the surface number density of chain ends with the decreasing M_n is not the same in the two M_n ranges. That is, the surface concentration of chain ends for a PS with M_n smaller than $10^{4.3}$ is not increased as effective as that for a PS with larger M_n even though M_n is decreased. Since T_g^s is strongly dependent on the surface concentration of chain ends as mentioned, it is envisaged that there exist two M_n regimes, where T_g^s decreases with M_n in a different manner. Thus, T_g^s of the PS did not monotonically but sigmoidally decreased with M_n, as shown in Figure 2.

An effect of the sample deformation, i.e., the scanning of a probe tip, on T_g^s must be reported for the sake of completeness. Figure 4 shows the temperature dependence of dynamic loss modulus, E'', for the bulk PS sample with M_n of 1800K as a function of the measuring frequency, f, measured by a Rheovibron. The peaks on

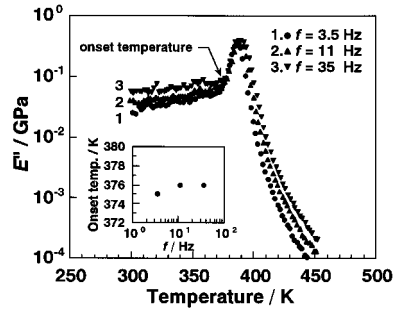

Figure 4. Dependence of dynamic loss tangent on temperature for the bulk PS with M_n of 1800K as a function of the measuring frequency. The inset shows an effect of frequency on the onset temperature.

the E''−temperature curves are assigned to the α_a absorption corresponding to the micro-Brownian motion of polymeric chains.[31] The inset of Figure 4 shows the frequency dependence of the onset temperature, at which the magnitude of E'' starts to increase. The inset makes it clear that the onset temperature is almost constant in the frequency range studied here. To combine our LFM results with a well-defined bulk mechanical properties such as E'', the scanning rate, v, of the LFM measurement was converted to the frequency corresponding to the bulk measurement, which was proportional to the inverse of a deformation period, as given by

$$f = v/2a \tag{3}$$

where a is the contact radius of the tip. According to Johnson−Kendall−Roberts (JKR) theory, which counts the surface force effect on contact phenomena between two elastic bodies,[32] a is expressed as follows:

$$a^3 = \frac{R_t}{K}\left\{F_c + 3\pi R_t W_{12} + \sqrt{6\pi R_t F_c W_{12} + (3\pi R_t W_{12})^2}\right\} \tag{4}$$

R_t, K, F_c, and W_{12} are the radius of curvature of a tip, the converted modulus, the contact force, and the adhesive work, respectively. Although it is difficult to estimate the precise magnitudes of all variables in eq 4 for the moment, f can be roughly estimated to be 70 Hz by using reasonable numbers. Since the sample deformation rate dependence of the onset temperature does not exist apparently in this frequency region, as shown in the inset of Figure 4, it seems reasonable to claim here that the discrepancy between T_g^s and T_g^b displayed in Figure 2 does not arise from the sample deformation.

Next, it is shown how lateral force changes as a function of scanning rate of a tip on the PS surface at different temperatures. Figure 5 shows the relationships between scanning rate and lateral force on the PS films with M_n of (a) 4.9K and (b) 140K at different temperatures. In both PS films, the lateral force was independent of the scanning rate at a lower temperatures such as 259 and 325 K for PS with M_n values of 4.9K and 140K, respectively, as shown at the bottoms of Figure 5, parts a and b. It should be noted once again that the lateral force is invariant across two decades in the scanning rate if the surface is in a glassy state. Figure 5 shows that both surfaces with M_n values of 4.9K and 140K are in the glassy state up to about 259 and 325 K. These are in good accord with the results presented earlier that T_g^s with M_n values of 4.9K and 140K are

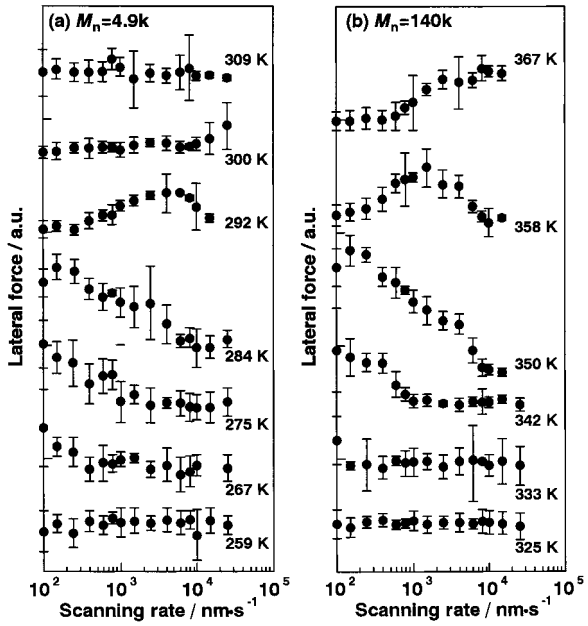

Figure 5. Scanning rate dependence of the lateral force with various temperatures for the monodisperse PS films with M_n of 4.9K and 140K.

267 and 335 K, as shown in Figure 2. When the measurement was carried out at higher temperatures, e.g., from 267 to 275 K and from 333 to 342 K for the PS films with M_n values of 4.9K and 140K, respectively, the lateral force increased with decreasing scanning rate, especially at the lower scanning rates. Further, the lift-off point on the lateral force−scanning rate curve was shifted to the higher scanning rates. As the PS film was heated, a peak was clearly observed on the lateral force−scanning rate curve. The peak appeared in the temperature ranges of 284−292 K and 350−367 K for the samples of 4.9K and 140K. At higher temperatures than 300 and 367 K for the samples of 4.9K and 140K, the lateral force decreased with decreasing scanning rate. Eventually, the lateral force recovered the invariance with respect to the scanning rate, and this is shown at the top of Figure 5a. Thus, the overall profiles reflect a successive change of the surface molecular motion from the glassy state to the rubbery state via the transition with the increasing temperature. Since the performance of the piezoscanner was not stable at a temperature higher than 373 K, the LFM measurement for the PS with M_n of 140K was truncated at 367 K. The shape of each curve in Figure 5 suggests that the master curves for the lateral force−scanning rate relation might be obtained by the horizontal and vertical shifts. Since the error bar was not necessarily small, only the horizontal shift, a_T, was quantitatively evaluated.

Figure 6 shows the master curves for the PSs with M_n of 4.9K and 140K drawn by horizontal and vertical shifts of each curve shown in Figure 5 as the reference temperatures of 267 and 333 K, respectively. The amount of horizontal shift, namely, the shift factor, a_T, is collected in Table 1. The master curves obtained from the dependence of lateral force on the scanning rate was very similar to the lateral force−temperature curves, as shown in Figure 1. Therefore, it seems reasonable to consider as a general concept that the scanning rate dependence of the lateral force exhibits a peak in a glass−rubber transition, and that the lateral force in a glassy and a fully rubber regions is independent of the

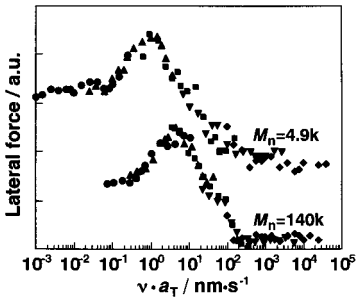

Figure 6. Master curves of the scanning rate-lateral force relationship for the PS films with M_n of 4.9K and 140K drawn from the each curve in Figure 5. Reference temperatures of 267 and 333 K were used for the PSs with M_n of 4.9K and 140K, respectively.

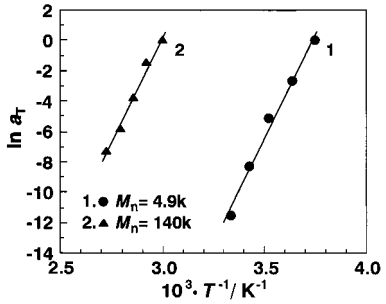

Figure 7. Semilogarithmic plots of shift factor, a_T, vs reciprocal absolute temperature for the PS films with M_n of 4.9K and 140K.

Table 1. Shift Factors, a_T, for PSs with M_n of 4.9K and 140K

T/K	a_T	T/K	a_T
	(a) M_n = 4.9K		
267	1.0	292	2.5×10^{-4}
275	7.0×10^{-2}	300	1.0×10^{-5}
284	6.0×10^{-3}		
	(b) M_n = 140K		
333	1.0	358	3.0×10^{-3}
342	2.3×10^{-1}	367	7.0×10^{-4}
350	2.3×10^{-2}		

scanning rate. It is clear from Figure 6 that the time−temperature superposition principle, which is characteristic of bulk viscoelastic materials, can be applied to the surface relaxation process as well. Assuming that a_T, has a functional form of Arrhenius type,[33,34] the apparent activation energy for the α_a-relaxation process, $\Delta H^{\ddagger}$, is given by

$$\ln a_T = \frac{\Delta H^{\ddagger}}{R}\left(\frac{1}{T} - \frac{1}{T_o}\right) \tag{5}$$

where R is the gas constant and T and T_o are the measuring and the reference temperatures, respectively. Figure 7 shows the relationships between ln a_T and the reciprocal absolute temperature for the PSs with M_n values of 4.9K and 140K, the so-called Arrhenius plots. The activation energy for the surface α_a-relaxation process calculated from each slope of Figure 7 was 230 ± 10 kJ·mol^{-1}, independent of M_n for the PS. This magnitude was much smaller than the reported values for bulk PS sample, ranging from 360 to 880 kJ·mol^{-1}.[35,36] The cooperative length scale of micro-Brownian motion for a fragile glass near T_g^b has been reported to be approximately 2 nm.[37] That is, a segment existing in the surface region of 2 nm from the outermost surface

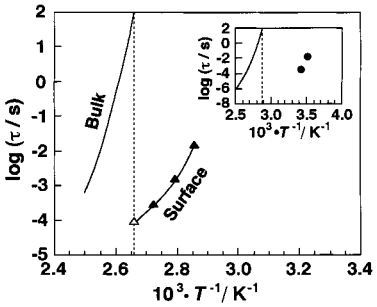

Figure 8. Semilogarithmic plot of segmental relaxation time against reciprocal absolute temperature for the PS film with M_n of 140K. The solid line denotes the log $\tau - 10^3/T$ relation for the corresponding bulk PS calculated from Vogel−Fulcher equation. The vertical dashed line merely denotes T_g^b. The filled and open triangles are the experimental relaxation times at the surface and calculated one at T_g^b by extrapolating experimental surface τ, respectively. The inset is the same plot for the PS film with M_n of 4.9K, provided that the experimental surface τ values are represented by filled circles.

is supposed to have a fewer neighbor segments to move cooperatively. The analytical depth of our LFM measurement might be smaller than 1 nm,[38] and thus the surface $\Delta H^{\ddagger}$ was remarkably smaller than the reported values for bulk PS, resulting in the observation that the T_g^s was also lower than the T_g^b even for the infinite M_n PS. To make quantitative evaluation of the cooperativity at the PS surface, the coupling model[39] proposed by Ngai et al. is applied to our results.

The correlation function of the motion after t_c, in which an intermolecular coupling between the local segmental motions in different chains starts to be cooperative, is given by eqs 6 and 7, where τ_1 is the

$$\phi(t) = \exp\left\{-\left(\frac{t}{\tau}\right)^{1-n}\right\} \tag{6}$$

$$\tau = \{t_c^{\,-n}\tau_1\}^{\{1/(1-n)\}} \tag{7}$$

single chain independent relaxation and n is the coupling parameter indicating cooperativity. The n for bulk PS was reported to be about 0.64.[40]

The main plot and the inset of Figure 8 show the semilogarithmic plots of the segmental relaxation time, τ, against $1/T$ for the PSs with M_n of 140K and 4.9K, respectively. The τs at the surface, filled symbols, were obtained on the basis of the scanning rate dependence of lateral force at a given temperature as shown in Figure 5. Since the peak scanning rate can be converted to the peak frequency by using eq 4, it is possible with the relation $\tau(2\pi f_{max}) = 1$ to evaluate the surface τ at a given temperature. The segmental relaxation time for bulk PS, which was calculated from Vogel−Fulcher equation, is also displayed in Figure 8 to compare with the surface τ.

$$\tau = \tau_o \exp\left(\frac{B}{T - T_V}\right) \tag{8}$$

In eq 8, the preexponential, a vibrational lifetime, of 10^{-14} s [36] and the activation temperature, B, of 1842 K were used. Also the Vogel temperature, T_V, was taken as (T_g^b− 50) K. It is apparent from Figure 8 that a segment located at the surface can be relaxed much faster than that in bulk. The same trend can be seen for the PS with M_n of 4.9K, as shown in the inset of

Figure 8. To estimate the coupling parameter at the surface using eq 7, it is necessary to know the τ and the τ_1 at a given temperature. Since the τ_1 is relaxation time of a single chain without the intermolecular interactions, it should be the same at the surface and in bulk. The τ_1 could be easily calculated at T_g^b, and its magnitude was $10^{-6.8}$ s.[39] Also, the surface τ at T_g^b was estimated to be 9.03×10^{-5} s by extrapolating three filled triangles to T_g^b. This surface τ was represented as a open triangle in Figure 8. Finally, the coupling parameter at the PS surface was found to be approximately 0.2, which was intensively smaller than the bulk value of 0.64. Thus, it seems reasonable to conclude that the size and/or energy barrier of the cooperative motion at the surface is much smaller than that in its internal bulk state. The apparent activation energy of the α_a-relaxation differs by a factor of 1.5−4 between the surface and the bulk, and the same factor seems to emerge for the difference in the cooperativity parameter n. This agreement may not be entirely accidental but may indicate a connection between the apparent activation energy and the degree of cooperativity in the context of Ngai's model. A reduction of the cooperativity at the surface might be seen to arise from the existence of the free space on the polymer surface.

Conclusions

The temperature-dependent LFM was applied to the examination of surface relaxation processes for the monodisperse PS films. T_g^s was found to be much lower than T_g^b in the entire M_n range. The M_n dependence of T_g^s was analyzed on the basis of Mayes' scaling prediction and a simple power law. Consequently, the exponent of M_n related to T_g^s was -0.60 ± 0.03 in contrast to the power of -0.5 from the Mayes' scaling theory assuming that both chain ends were perfectly localized at the surface. This result implies that the surface localization of end groups of the PS used here is not perfect. The T_g^s extrapolated to the infinite M_n was found to be lower than that for the bulk sample by approximately 20 K. It was shown that the well-established time−temperature superposition principle was applicable to the surface α_a-relaxation process as well. The apparent activation energy for the α_a-relaxation at the PS surface was calculated to be 230 ± 10 kJ·mol^{-1}, which was remarkably smaller than the reported values for bulk PS. The size of the cooperative movement at the surface was discussed on the basis of the Ngai's coupling model. As a result, it was shown that the cooperativity at the surface was intensively reduced in comparison with its interior bulk region. Finally, it was envisaged that the thermal molecular motion at the PS surface was activated by not only the surface localization of chain end groups but also the reduced cooperativity.

Acknowledgment. K.T. is most grateful for helpful discussions with our colleagues Kazuya Noda and Noriaki Satomi. This was in part supported by a Grant-in-Aid for Scientific Research (A) (#10355035) and COE Research (#08CE2005) from the Ministry of Education, Science, Sports, and Culture, Japan.

References and Notes

(1) Garbassi, F.; Morra, M.; Occhiello, E. *Polymer Surfaces, from Physics to Technology*; Wiley: Chichester, England, 1994.
(2) Beaucage, G.; Composto, R.; Stein, R. S. *J. Polym. Sci., Polym. Phys. Ed.* **1993**, *31*, 319.
(3) Reiter, G. *Macromolecules* **1994**, *27*, 3046.
(4) Keddie, J. L.; Jones, R. A. L.; Cory, R. A. *Europhys. Lett.* **1994**, *27*, 59.
(5) Forrest, J. A.; Dalnoki-Veress, K.; Stevens, J. R.; Dutcher, J. R. *Phys. Rev. Lett.* **1996**, *77*, 2002.
(6) Fukao, K.; Miyamoto, Y. *Phys. Rev. E* **2000**, *61*, 1743.
(7) Dalnoki-Veress, K.; Forrest, J. A.; de Gennes, P. G.; Dutcher, J. R. *J. Phys. IV* **2000**, *10*, 221.
(8) Kajiyama, T.; Tanaka, K.; Ohki, I.; Ge, S.-R.; Yoon, J.-S.; Takahara, A. *Macromolecules* **1994**, *27*, 7932.
(9) Tanaka, K.; Taura, A.; Ge, S.-R.; Takahara, A.; Kajiyama, T. *Macromolecules* **1996**, *29*, 3040.
(10) Kajiyama, T.; Tanaka, K.; Takahara, A. *Macromolecules* **1997**, *30*, 280.
(11) Satomi, N.; Takahara, A.; Kajiyama, T. *Macromolecules* **1999**, *32*, 4474.
(12) Tanaka, K.; Takahara, A.; Kajiyama, T. *Macromolecules* **1997**, *30*, 6626.
(13) Tanaka, K.; Jiang, X.; Nakamura, K.; Takahara, A.; Kajiyama, T.; Ishizone, T.; Hirao, A.; Nakahama, S. *Macromolecules* **1998**, *31*, 5148.
(14) Kajiyama, T.; Tanaka, K.; Satomi, N.; Takahara, A. *Macromolecules* **1998**, *31*, 5150.
(15) Terada, N.; Harada, M.; Ikehara, T.; Nishi, T. *J. Appl. Phys.* **2000**, *87*, 2803.
(16) Hammerschmidt, J. A.; Gladfelter, W. L.; Haugstad, G. *Macromolecules* **1999**, *32*, 3360.
(17) Boiko, Y. M.; Prud'homme, R. E. *J. Polym. Sci., Polym. Phys. Ed.* **1998**, *36*, 567.
(18) Jean, Y. C.; Zhang, R. W.; Cao, H.; Yuan, J. P.; Huang, C. M.; Nielsen, B.; Asoka-Kumar, P. *Phys. Rev. B* **1997**, *56*, R8459.
(19) Liu, Y.; Russell, T. P.; Samant, M. G.; Stöhr, J.; Brown, H. R.; Cossy-Favre, A.; Diaz, J. *Macromolecules* **1997**, *30*, 7768.
(20) Minato, K.; Takemura, T. *Jpn. J. Appl. Phys.* **1967**, *6*, 719.
(21) Mayes, A. M. *Macromolecules* **1994**, *27*, 3114.
(22) Fox, T.; Flory, P. *J. Polym. Sci.* **1954**, *14*, 315.
(23) Satomi, N.; Yokoe, Y.; Tanaka, K.; Takahara, A.; Kajiyama, T. Manuscript in preparation.
(24) Ballard, D. G. H.; Wignall, G. D.; Schelten, J. *Eur. Polym. J.* **1973**, *9*, 965.
(25) Mansfield, K. F.; Theodorou, D. N. *Macromolecules* **1991**, *24*, 6283.
(26) Doruker, P.; Mattice, W. L. *J. Phys. Chem. B* **1999**, *103*, 178.
(27) Yethiraj, A. *Chem. Eng. J.* **1999**, *74*, 109.
(28) Brown, H. R.; Russell, T. P. *Macromolecules* **1996**, *29*, 798.
(29) Legrand, D. G.; Gains, G. L. *J. Colloid Interface Sci.* **1969**, *31*, 162.
(30) Sperling, L. H. *Introduction to Physical Polymer Science*, 2nd ed.; Wiley: New York, 1992.
(31) Illers, K. H.; Jenckel, E. *Rheol. Acta* **1958**, *1*, 322.
(32) Johnson, K. L.; Kendall, K.; Roberts, A. D. *Proc. R. Soc. London A* **1971**, *324*, 301.
(33) Takayanagi, M. *Proceedings of the 4th Congress on Rheology*; Butterworth: London, 1965; p 161.
(34) Bueche, F. *J. Appl. Phys.* **1955**, *26*, 738.
(35) McCrum, N. G.; Read, B. E. *Anelastic and Dielectric Effects in Polymeric Solids*; Dover: New York, 1967.
(36) Santangelo, P. G.; Roland, C. M. *Macromolecules* **1998**, *31*, 4581.
(37) Ngai, K. L.; Rizos, A. K. *Mater. Res. Soc. Symp. Proc.* **1997**, *455*, 147.
(38) The indentation depth of a probe tip under the current experimental condition was calculated on the basis of JKR theory. It might increase drastically at a temperature higher than T_g^s due to decreasing surface modulus.
(39) Ngai, K. L.; Rizos, A. K.; Plazek, D. J. *J. Non-Cryst. Solids* **1998**, *235*, 435.
(40) Linsey, C. P.; Patterson, G. D.; Stevens, J. R. *J. Polym. Sci., Polym. Phys. Ed.* **1979**, *17*, 1547.

MA000406W